Fluctuation effects on chemical wave fronts

M. A. Karzazi,[1] A. Lemarchand,[1] and M. Mareschal[2]
[1]*Université Pierre et Marie Curie, Laboratoire de Physique Théorique des Liquides, CNRS URA No. 765, 4, place Jussieu, 75252 Paris Cedex 05, France*
[2]*Université Libre de Bruxelles, Service de Chimie-Physique, Case Postale 231, Boulevard du Triomphe, 1050 Bruxelles, Belgium*
(Received 28 May 1996)

The numerical resolution of the Langevin equations, with specific internal noises deduced from master equations, exhibits two qualitatively different behaviors for the reaction-diffusion wave fronts associated with either a cubic or a quadratic chemical rate. In the case of a wave front between two stable stationary states, illustrated by the Schlögl model, the effect of fluctuations in the vicinity of a bifurcation induces perturbative deviations from the deterministic predictions on observable properties, like the propagation velocity, the profile width, and the value of the highest plateau. These deviations obey power laws that are determined. For wave fronts propagating into an unstable stationary state, such as in the Fisher model, a nonperturbative fluctuation effect on velocity and profile width is observed, in relation to the selection, in the presence of noise, of a particular solution in the continuum of linearly stable deterministic solutions. [S1063-651X(96)03010-3]

PACS number(s): 47.70.Fw, 82.20.−w, 05.40.+j

I. INTRODUCTION

The macroscopic description of spatiotemporal patterns [1–3] in nonhomogeneous chemical systems involves partial differential equations, also encountered in various domains ranging from biology to physics or economics. We are interested here in the propagation of wave fronts [1–11] defined as uniformly translating solutions of reaction-diffusion equations, replacing a homogeneous stationary state by another homogeneous stationary state. A wave front appears as a stationary spatial structure in an appropriate moving frame.

In the framework of population dynamics, Fisher [4] and Kolmogorov, Petrovski, and Piskunov [5] introduced at the same time a simple model in order to describe the propagation of a favored genetic character through a population. This model, further referred as the Fisher model for the sake of briefness, is associated with a quadratic chemical rate. The corresponding reaction-diffusion equation admits wave-front solutions propagating between a stable stationary state and an unstable stationary state. Reducing the dynamics to the evolution in the frame moving at the wave-front velocity, a linear stability analysis of the wave front does not lead to the selection of a unique stable solution. It prescribes only a lower bound to a continuous velocity spectrum associated with the set of linearly stable solutions [4–9]. Later, Schlögl, Escher, and Berry [10] proposed a different chemical model associated with a cubic kinetics in order to compare bistability in nonequilibrium systems and the liquid-gas transition. The Schlögl model has been specially designed to give rise to a pitchfork bifurcation, in many respects analogous to the second order phase transition observed during the liquefaction of a gas in the vicinity of the critical point. Depending on the parameter values, the reaction-diffusion equation associated with the Schlögl model admits either one or three homogeneous stationary states. In this last case, it possesses a unique stable wave-front solution connecting the two stable stationary states [10,11]. Contrary to the Fisher case, the dynamics prescribes a well-defined and unique propagation velocity.

Our aim is not to apply these models to specific physical problems but to use them as generic situations, and to discuss the validity of the macroscopic deterministic description of the two different wave-front types they generate. Actually, reducing the dynamics of a large number of individuals to the deterministic evolution of macroscopic variables requires a strong assumption about the range of statistical correlations that we are now able to test, thanks to the improvement of computational tools. Whatever the nature of the elementary systems considered, whether it consists of molecules, living beings, or financial assets, their microscopic dynamics generates fluctuations around the statistical mean behavior which may induce observable deviations to the predicted deterministic behavior.

Near a transition, fluctuations developing in equilibrium systems are amplified so as to reach a macroscopic level leading for example to the opalescence of a fluid maintained in the vicinity of the critical point. Analogous phenomena are observed in nonequilibrium systems [12–14] for parameter values corresponding to a bifurcation. In this respect, the Schlögl model is certainly well suited to analyze the modifications of the wave-front properties when the three stationary states coalesce and when the effect of fluctuations is taken into account. The Fisher model illustrates an other degenerate situation, where the fluctuations are supposed to play a major role. Indeed, the existence of a continuum of propagation velocities associated with linearly stable wave fronts may enhance the sensitivity to fluctuations, and it may be asked whether internal noise influences the selection of a particular propagation velocity in the spectrum.

The two types of reaction-diffusion wave fronts have already been studied using lattice-gas cellular automata (LGCA) [15–22], the master equation [23–26] or Monte Carlo simulations [23,24,27], and stochastic partial differential equations [28,29]. Hereafter, mean refers to a time average of a front property for a given initial condition, and for an approach including the description of fluctuations. Up to now, discrepancies between mean wave-front properties and corresponding deterministic predictions have only been ob-

served in the case of the Fisher model, using stochastic partial differential equations [29] to take internal noise into account. Moreover, the quantitative determination of the deviation dependence on the fluctuation amplitude was limited to the propagation velocity.

In the present work, we choose to describe the internal fluctuations at a mesoscopic level. Adopting the Langevin formalism, our stochastic approach [29] amounts to adding specific noise terms to the deterministic partial differential equations. The noise statistics, deduced from a master equation [12–14] and then reduced to a Gaussian distribution, is designed to reproduce the macroscopic consequences of the internal fluctuations. From an analysis of fluctuation effects, we intend to deduce quantitative characteristics allowing for a classification of the different wave-front types. Knowing that, in the case of the wave front associated with the Fisher model, the velocity deviation from the deterministic prediction varies like a power of the fluctuation amplitude [29], we wish to determine if an analogous behavior is also observed for the different wave-front type associated with the Schlögl model. We then intend to compare the exponent values of the scaling laws. Contrary to microscopic simulations [15–22,27], the mesoscopic approach used here consists of the numerical resolution of stochastic equations. It preserves the analytical character of the description, and makes easier a comparison with the deterministic analysis. In particular, the parameters of the deterministic equations appear also in the stochastic description contrary to the case of LGCA [21]. In such microscopic simulations, the relation between microscopic and deterministic parameters is not always obvious, and the precision of its determination limits the accuracy of the results concerning the wave front. Nevertheless, the ability of the Langevin approach to reproduce faithfully the consequences of the underlying microscopic dynamics needs to be checked. Up to now, the equivalence of the Langevin formalism and a microscopic simulation based on LGCA has been proved with regard to the geometrical properties of wave fronts [30]. Indeed, we obtain an excellent agreement between the fractal dimensions of two-dimensional (2D) wave fronts deduced from the two different methods.

II. TWO TYPES OF REACTION-DIFFUSION WAVE FRONTS

We analyze two different chemical models, corresponding either to a quadratic or a cubic chemical rate, respectively known as the Fisher model [1–9] and the Schlögl model [10,11]. In each case, we consider an infinite one-dimensional (1D) medium containing different chemical species that diffuse with an identical coefficient D.

The Fisher model [1–9] involves two species A and B, reacting according to the following autocatalytic step of rate constant K:

$$A+B\rightarrow 2A. \tag{1}$$

Since reaction (1) keeps constant the total number of particles, the local macroscopic concentrations, $A(x,t)$ and $B(x,t)$, obey

$$\overline{A}(x,t)+\overline{B}(x,t)=C, \tag{2}$$

where C is constant so that the deterministic evolution of the system reduces to a single partial differential equation for the dimensionless fraction $\overline{a}\equiv\overline{a}(x,t)=A(x,t)/C$:

$$\frac{\partial\overline{a}}{\partial t}=KC\overline{a}(1-\overline{a})+D\frac{\partial^2\overline{a}}{\partial x^2}, \tag{3}$$

with $0\leqslant\overline{a}\leqslant 1$, and where t is time and x the spatial coordinate.

The reaction-diffusion equation (3) admits uniformly translating solutions, $\overline{a}(x-Vt)$, moving with a constant velocity V and replacing the unstable uniform stationary state $\overline{a}=0$ by the stable state $\overline{a}=1$. A linear stability analysis around such wave-front solutions in the moving frame at velocity V does not allow for the selection of a given velocity. Indeed, an essential feature [1–9] of Eq. (3) is the existence of linearly stable solutions for any propagation velocity V greater than a minimum value V given by

$$\overline{V}=2\sqrt{KCD}. \tag{4}$$

Mathematical results [6] state that a large class of sufficiently steep initial profiles evolve in time to the stable solution $\overline{a}(x-Vt)$ propagating with this minimum allowed velocity. The analytical expression of the stationary profile propagating at velocity V is not known, but a practical measure of its width E may be deduced from the approximate value [2] of the steepness at the inflection point. One has

$$\overline{E}=8\left(\frac{D}{KC}\right)^{1/2}. \tag{5}$$

The Schlögl model [10,11] involves a single species A of variable concentration $A(x,t)$ that reacts with species C_1 and C_2 of constant concentrations according to

$$\begin{gathered} C_1+2A\underset{K_{-1}}{\overset{K_1}{\rightleftharpoons}}3A, \\ A\underset{K_{-2}}{\overset{K_2}{\rightleftharpoons}}C_2. \end{gathered} \tag{6}$$

For appropriate values of the parameters K_1, K_{-1}, K_2, K_{-2}, C_1, and C_2, the cubic chemical rate admits two stable and an unstable stationary states. The deterministic equation for the dimensionless variable $\overline{a}\equiv\overline{a}(x,t)=A(x,t)/C$, where $C=C_1+C_2$ is constant, may be written as

$$\frac{\partial\overline{a}}{\partial t}=-K_{-1}C^2(\overline{a}-\alpha)(\overline{a}-\beta)(\overline{a}-\gamma)+D\frac{\partial^2\overline{a}}{\partial x^2}, \tag{7}$$

with $\alpha\geqslant\beta\geqslant\gamma\geqslant 0$. Contrary to the Fisher case, the variable $\overline{a}$ is not bounded from above. Equation (7) admits a single wave front connecting the two stable stationary states $\overline{a}=\alpha$ and $\overline{a}=\gamma$:

$$\overline{a}(z)=\alpha+\frac{\gamma-\alpha}{1+e^{-4z/\overline{E}}}, \tag{8}$$

where $z=x-\overline{V}t$, and where the width $\overline{E}$ deduced from the steepness at the inflection point obeys

$$\overline{E}=\frac{4\sqrt{2}}{\alpha-\gamma}\left(\frac{D}{K_{-1}C^2}\right)^{1/2}. \tag{9}$$

Another important difference with Eq. (3) associated with the Fisher model is that, for the Schlögl front, the propagation velocity V is uniquely prescribed by the dynamics (11), and given by

$$\overline{V}=\left(\frac{K_{-1}C^2D}{2}\right)^{1/2}(\alpha+\gamma-2\beta). \tag{10}$$

Here we impose the condition

$$\beta<\frac{\alpha+\gamma}{2}, \tag{11}$$

so that the propagation velocity will be positive as for the Fisher front.

The Fisher and the Schlögl models may be considered as prototypes of the two classes of reaction-diffusion fronts either propagating into an unstable stationary state replaced by a stable one or connecting two stable states. In order to make more relevant the comparison between the two models, we choose

$$\gamma=0 \tag{12}$$

for the Schlögl model so that the same state, $\overline{a}=0$, is imposed for $z\rightarrow+\infty$.

III. MESOSCOPIC DESCRIPTION OF THE INTERNAL FLUCTUATIONS

We have recently proved [29], in the case of the wave front associated with the Fisher model, that the internal fluctuations may induce macroscopic deviations from the results predicted by a deterministic description of the dynamics. In Ref. [29], the statistics deduced from a multivariate master equation was first reduced to a Gaussian distribution. The corresponding Langevin equations were then numerically solved. We observed an increase of the mean wave-front propagation velocity up to 25%. We now wish to use the same method to compare the behavior of the two wave-front types. In this respect, it is first necessary to improve the precision of the results obtained in the case of the Fisher wave front for the propagation velocity, and then to characterize quantitatively the fluctuation effects on the front width. Finally, the same kind of analysis has to be adapted to the Schlögl model.

We first briefly recall the main steps of our stochastic analysis [29] derived from the master equation [12–14]. This latter gives the evolution of the probability of the fraction $a(x,t)$ of particles A, considered as a random variable. The chemical reaction is modeled by birth and death processes and diffusion by a random walk. The master equation lays on a spatial discretization into cells. The choice of the cell length Δl is a balance between two opposite constraints. On the one hand, the cells must be sufficiently small to be considered as homogeneous. On the other hand, a proper description of the chemical processes inside a cell requires sufficiently large cells containing a large number N of molecules. This latter condition justifies a system-size expansion [13] of the master equation to the first order in $1/N$. Within a Gaussian approximation, irreductible transition moments of orders higher than 2 are neglected. The effect of the fluctuations may be reproduced by adding a Langevin force to the deterministic equations. The mean and variance of this force define on their own the whole statistics. The Langevin force amplitude [14] is governed by the size of the system and is proportional to $1/\sqrt{N}$. In order to control the fluctuation amplitude while maintaining constant the concentration C, we introduce a spatial scaling factor ν, fixing the size of a cell by

$$\Delta l=\nu\Delta l_0, \quad N=\nu N_0, \tag{13}$$

where Δl_0 and N_0 are reference values.

We define discrete space and time variables by

$$i=\frac{x}{\Delta l}, \quad s=\frac{t}{\Delta t}, \tag{14}$$

where i and s are integers, and where Δt is the time step.

Introducing dimensionless parameters

$$k=KC\Delta t, \tag{15}$$

$$\frac{d}{\nu^2}=\frac{D\Delta t}{(\nu\Delta l_0)^2}, \tag{16}$$

the discrete Langevin equations associated with the Fisher model [29], for cells of length Δl containing in average N particles, are given by

$$\begin{aligned}a_i(s+1)=a_i(s)+ka_ib_i+\frac{d}{\nu^2}(a_{i+1}+a_{i-1}-2a_i)\\+\left(\frac{k}{\nu N_0}\right)^{1/2}\sqrt{\overline{a_i}(1-\overline{a_i})}Y_i(s)\\+\left(\frac{d}{\nu^3N_0}\right)^{1/2}[\sqrt{\overline{a_{i-1}}+\overline{a_i}}Z_i^a(s)\\-\sqrt{\overline{a_{i+1}}+\overline{a_i}}Z_{i+1}^a(s)],\end{aligned} \tag{17}$$

$$\begin{aligned}b_i(s+1)=b_i(s)-ka_ib_i+\frac{d}{\nu^2}(b_{i+1}+b_{i-1}-2b_i)\\+\left(\frac{k}{\nu N_0}\right)^{1/2}\sqrt{\overline{a_i}(1-\overline{a_i})}Y_i(s)\\+\left(\frac{d}{\nu^3N_0}\right)^{1/2}[\sqrt{2-\overline{a_{i-1}}-\overline{a_i}}Z_i^b(s)\\-\sqrt{2-\overline{a_{i+1}}-\overline{a_i}}Z_{i+1}^b(s)],\end{aligned} \tag{18}$$

where $Y_i(s)$, $Z_i^a(s)$, and $Z_i^b(s)$ are independent Gaussian white noises of zero mean and unit variances obeying, in particular,

$$\langle Z_i^a(s)Z_{i'}^b(s')\rangle=\delta_{ab}\delta_{ii'}\delta_{ss'}. \tag{19}$$

Contrary to the deterministic case where the fractions are linked by $\overline{a}(x,t)+b(x,t)=1$, the stochastic description cannot be reduced to a single Langevin equation but requires the

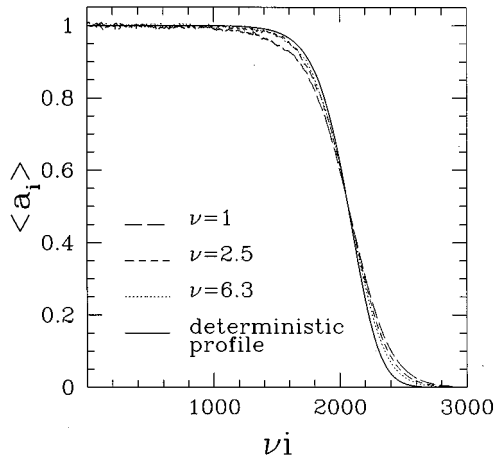

FIG. 1. Mean Fisher wave-front profiles $\langle a_i \rangle$, solutions of the Langevin equations in the moving frame for different values of the spatial scaling factor ν. The cell number is denoted by i. The results are obtained for the following parameter values: $n=4096$, $N_0=100$, $\Delta l_0=1$, $\Delta t=1$, $d=0.2$, and $k=5.12\times10^{-5}$.

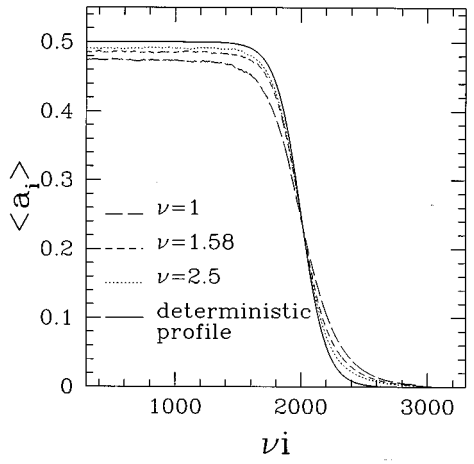

FIG. 2. Same caption as Fig. 1 for the Schlögl model and the following parameter values: $n=4096$, $N_0=100$, $\Delta l_0=1$, $\Delta t=1$, $d=0.2$, $k=1.6\times10^{-4}$, $\alpha=0.5$, $\beta=10^{-3}$, and $\gamma=0$.

resolution of two coupled equations for the fractions a and b of particles A and B, respectively. At this lower order of the system-size expansion, we have replaced the fractions a and b in the Langevin force expressions by their deterministic values $\overline{a}$ and $\overline{b}$. At the end of Sec. IV we shall come back to the consequences of this approximation.

For the Schlögl model, the dimensionless diffusion coefficient d is also given by Eq. (16), whereas the dimensionless rate constant k obeys

$$k=K_{-1}C^2\Delta t. \tag{20}$$

The discrete Langevin equation for $a_i(s+1)$ may be written as

$$\begin{aligned} a_i(s+1)=a_i(s)-ka_i(a_i-\alpha)(a_i-\beta)+\frac{d}{\nu^2}\,(a_{i+1}+a_{i-1} \\ -2a_i)+\left(\frac{k}{\nu N_0}\right)^{1/2}\sqrt{\overline{a_i}(\overline{a_i}+\alpha)(\overline{a_i}+\beta)}\,Y_i(s) \\ +\left(\frac{d}{\nu^3 N_0}\right)^{1/2}[\sqrt{\overline{a_{i-1}}+\overline{a_i}}Z_i(s) \\ -\sqrt{\overline{a_{i+1}}+\overline{a_i}}Z_{i+1}(s)]. \end{aligned} \tag{21}$$

For each model, Eqs. (17), (18), and (21) are numerically solved. We thus follow the evolution in discrete time s of the fraction $a_i(s)$ and $b_i(s)$ in each cell i. The total number of cells, n, in the 1D medium considered is typically equal to 4096. The deterministic profile is chosen as initial condition. Imposing Eq. (11) for the Schlögl model, the propagation velocity is positive. For the Fisher model, it is positive without condition. Consequently, the chemical reactions tend to increase the total fraction of particules A in the entire system for the two models. Particular boundary conditions [29] are imposed in order to mimic an infinite medium. At each time step s, where

$$\sum_{i=1}^{n} a_i(s) > \sum_{i=1}^{n} a_i(0), \tag{22}$$

the A excess is reduced by suppressing the first cell and creating a last cell in which $a_n(s)=0$. At the same time, the front position $\phi(s)$ is increased by Δl. For the parameter values considered, this procedure occurs only every 10^3 time steps in average. Typically, it amounts to switch into the frame moving at the fluctuating front velocity V defined as the derivative of $\phi(s)$.

Depending on the spatial scaling factor ν, different asymptotic regimes are reached in the moving frame. It is then possible to define a mean stationary profile associated with a mean stationary velocity $\langle V \rangle$. The mean profile width $\langle E \rangle$ is deduced from the slope of the mean stationary profile at the inflection point. Note that the notion of stationarity loses its sense if the macroscopic properties of the front, like the profile width and the propagation velocity, are defined as square roots of the variances of the corresponding stochastic quantities [17–19,24–26].

IV. RESULTS

In this section, from the Langevin approach we deduce the mean properties of the two front types, and compare their deviations from the deterministic predictions. We begin with a qualitative description of the fluctuation effects on the mean wave-front properties.

The mean front profiles, solutions of the Langevin equations in the moving frame for different values of the spatial scaling factor ν, are given in Figs. 1 and 2 for the Fisher and Schlögl models, respectively. As ν decreases, the noise amplitude increases, and the profiles become smoother whatever the front type. They deviate more and more from the corresponding deterministic profiles and their mean width increases as well as the propagation velocity, as illustrated by the slopes of the curves in Figs. 3 and 4. In the case of the Schlögl model, a third effect is observed in Fig. 2: the mean fraction at the left boundary, $\langle a_{-\infty} \rangle$, does not tend to the stationary state value α, the deviation increasing as ν decreases. Since we imposed $\gamma=0$ and introduced deterministic

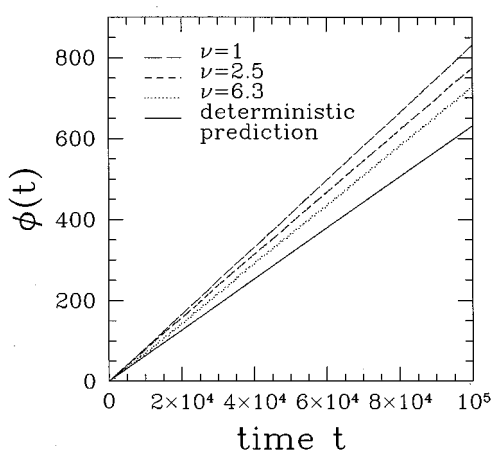

FIG. 3. Variation of the front position, $\phi(t)$, with time t in the fixed frame for Fisher's model and for different values of the spatial scaling factor ν. The parameter values are given in the Fig. 1 caption.

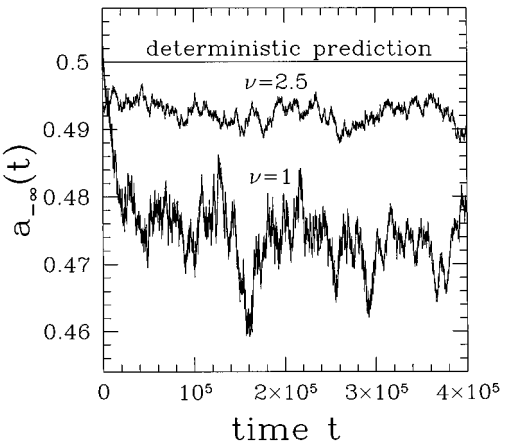

FIG. 5. Time evolution of the instantaneous left plateau value $a_{-\infty}(t)$ for the Schlögl model and for parameter values given in the Fig. 2 caption. The initial condition is the deterministic profile obeying $a_{-\infty}(t=0)=\alpha=0.5$.

fraction values in the noise expression given in Eq. (21), the fluctuations tend to zero in the leading edge of the front and do not affect the value at the left boundary obeying consequently $\langle a_{+\infty}\rangle=0$. Following the time evolution of the instantaneous profile width and left plateau height, from their initial value associated with the deterministic profile, allows us to determine when stationary conditions are reached in the moving frame. Figure 5 illustrates, in the Schlögl case, the decay of the left plateau value observed during the transient regime and followed by a stabilization around a well-defined mean value. The time evolutions of the left plateau value and profile width provide a convenient indication of the beginning of the permanent regime. Note that the results given in Figs. 1–4 have been determined once that stage has been reached.

It is to be noted that the effect of the fluctuations on the Fisher front exists whatever the choice of the two parameters k and d of the model. For the Schlögl model, the results are nearly independent of the parameter β. Conversely, a deviation from the deterministic predictions appears only for small values of the parameter α. We shall come back later to this point.

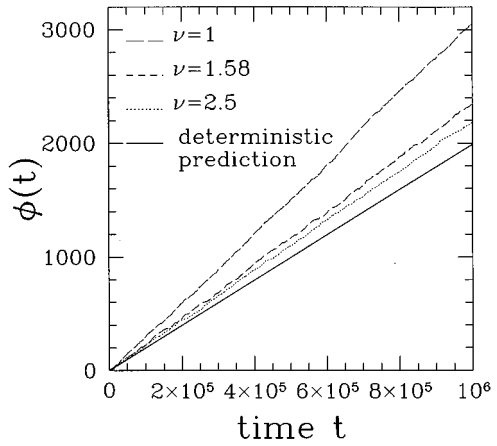

FIG. 4. Same caption as Fig. 3 for the Schlögl model and for parameter values given in the Fig. 2 caption.

We now wish to quantify the variations of the mean front properties with the fluctuation amplitude controlled by $1/N$. To remain in a domain of reasonable computation times, the number of spatial cells into which the 1D medium is divided does not exceed $n=4096$. Typically, the determination of the data appearing in Table I requires 1–2 h on a CRAY C98 supercomputer for each model. We choose the parameter values of the two models so that the width of the two profile types will be comparable, and will not exceed 20% of the medium length. This last precaution ensures that the somewhat artificial boundary conditions imposed do not perturb the front behavior too much. More precisely, we have checked that our results are independent of the number n of cells, provided n is not too small.

Let us sum up all the requirements limiting the choice of the five parameters of the Schlögl model: the left plateau height α must be sufficiently small (we choose $\alpha=0.5$); the unstable stationary state β obeys Eq. (11); the right plateau value γ vanishes; the diffusion coefficient obeys, whatever the spatial scaling factor ν, $d/\nu^2<0.25$, to ensure the convergence [31] of the algorithm used to solve Eq. (21) numerically; finally, the choice of a reasonable profile width, with respect to the total cell number in the medium, imposes the rate constant value, k. All these requirements lead to a propagation velocity smaller than in the Fisher case. To obtain a comparable accuracy in the velocity determination in both cases, it is consequently necessary to increase the integration time of the Langevin equation (21) associated with the Schlögl model.

The system-size expansion parameter $(1/N)$ is related to the spatial scaling factor ν through Eq. (13). The variation domains of $1/N$ and consequently $1/\nu$ are bounded. Indeed, the discrepancy between stochastic and deterministic descriptions becomes undetectable below a given threshold whereas the validity of the system-size expansion imposes an upper boundary. We observe that the wave front is destroyed when $1/N$ becomes too large, greater than $\frac{1}{50}$ for the values chosen here for the other parameters. The choice of $N=100$, illustrated in Table I, leads to the maximum reliable deviations from the deterministic predictions. For both velocity and width, the deviations exceed 30% for the two different

TABLE I. Maximum reliable deviations from deterministic predictions for the propagation velocity and the profile width. The results of the Langevin approach are given for the two front types propagating in a 1D medium. The parameter values have been chosen to lead to comparable width values. In each case, we impose $n=4096$, $N_0=100$, $\nu=1$, $\Delta l_0=1$, $\Delta t=1$, and $d=0.2$. The dimensionless rate constant k is fixed to 5.12×10^{-5} in the Fisher model, and to 1.6×10^{-4} in the Schlögl model.

	$10^3\,\overline{V}$	$10^3\,\langle V\rangle$	$\overline{E}$	$\langle E\rangle$	$\overline{a_{-\infty}}$	$\langle a_{-\infty}\rangle$
Fisher	6.300	8.336±0.002	500	655±5	1	1
Schlögl	1.990	3.020±0.005	400	605±5	$\alpha=0.5$	0.473±0.001

models. In Schlögl's case, the effect on the left plateau is always weak and remains smaller than 5%.

Figure 6 shows a log-log plot of the variations with the spatial scaling factor ν of the relative difference between the mean front properties deduced from the Langevin equations and the corresponding deterministic predictions. For both models, we have represented the relative velocity deviation $(\langle V\rangle-V)/V$ and the relative profile width deviation $(\langle E\rangle-E)/E$. For the Schlögl model, the ν dependence of the difference $(\langle a_{-\infty}\rangle-\alpha)/\alpha$ between the mean fraction at the left boundary, $\langle a_{-\infty}\rangle$, and the stable stationary state value α has been added.

For the Fisher model, we obtain the following power laws for the relative profile width deviation and the relative velocity deviation:

$$\left(\frac{\langle E\rangle-\overline{E}}{\overline{E}}\right)_F\sim\left(\frac{1}{N}\right)^{0.31\pm0.02}, \tag{23}$$

$$\left(\frac{\langle V\rangle-\overline{V}}{\overline{V}}\right)_F\sim\left(\frac{1}{N}\right)^{0.38\pm0.02}, \tag{24}$$

where the subscript F stands for Fisher.

The precision of the exponent determination is limited by the extension of the variation domain of $1/N$, here covering a decade and a half. Equation (24) provides confirmation of the existence of a scaling law [29] for the propagation velocity variation with the amplitude of the fluctuations, and improves the accuracy of the exponent determination. The result expressed by Eq. (23) is the existence of an analogous power law for the profile width variation with $1/N$. It is to be noted that the maximum relative deviations for velocity and width nearly coincide, as already observed in Table I. Moreover, the exponent values of the power laws associated with velocity and width are close and much smaller than 1. At the precision of the results, velocity and width vary in a similar way with the fluctuation amplitude. The existence of correlations between the fluctuations of the propagation velocity and the profile width, qualitatively observed [27] in microscopic simulations using a direct simulation Monte Carlo method [32], is very intuitive. Indeed, a small increase of the profile width improves the contact between the two reactive species A and B. It thus leads to an increase of the number of particles A produced by reaction (1), and consequently to an increase of the propagation velocity deduced from Eq. (22). Obtaining exponents smaller than 1 implies that the fluctuation effects on the mean wave-front properties cannot be considered as perturbative with respect to the system-size expansion parameter $1/N$.

For a sufficiently small value of the parameter α, in the case of the Schlögl model we have

$$\left(\frac{\langle E\rangle-\overline{E}}{\overline{E}}\right)_S\sim\left(\frac{1}{N}\right)^{1.38\pm0.02}, \tag{25}$$

$$\left(\frac{\langle V\rangle-\overline{V}}{\overline{V}}\right)_S\sim\left(\frac{1}{N}\right)^{1.39\pm0.02}, \tag{26}$$

$$\left(\frac{\langle a_{-\infty}\rangle-\alpha}{\alpha}\right)_S\sim\left(\frac{1}{N}\right)^{1.15\pm0.02}, \tag{27}$$

where the subscript S stands for Schlögl.

The same comments as in the Fisher case are also valid here for the fluctuation effect on velocity and width. However, the exponent values are much greater than for the Fisher model, and here exceed the value 1. In addition to the effect obtained on velocity and width, a third effect is observed in bistable systems on the left plateau value. As shown in Fig. 6, the deviation from the stationary state α also follows a power law. As already mentioned, the maximum deviation is weaker for the left plateau value than for velocity and width, but the slopes of the straight lines associated with the different properties are always greater than 1. The fluctuations in a bistable system induce a perturbative effect on the wave-front properties for close values of the three stationary states, i.e., close to a bifurcation point. Contrary to the Fisher case, the choice of a small value for the system-size expansion parameter $1/N$ ensures that the effect of fluctuations on the wave front will also be small. Moreover, far from a bifurcation, no fluctuation effect is observed.

The determination of the exponents is less accurate in Schlögl's case since the deviation decreases rapidly as $1/N$ decreases, according to the large exponent values. For the same accuracy in the property determination as in the Fisher model, the deviation between the deterministic predictions becomes sooner undetectable, explaining why the accessible variation domain of $1/N$ is smaller in Schlögl's case.

We recall that, for the Fisher model, the scaling laws given in Eqs. (23) and (24) are observed whatever the parameter values. Conversely, the effect of fluctuations disappears in the Schlögl model if the stationary state value α is too large. The existence of scaling laws given in Eqs. (25)–(27) are related to the deviation from the bifurcation of the cubic chemical rate associated with the coalescence of the three stationary states α, β, and $\gamma=0$. Note that, for a given value of α, the effects we observe are nearly independent of the unstable stationary state β. In order to make explicit the

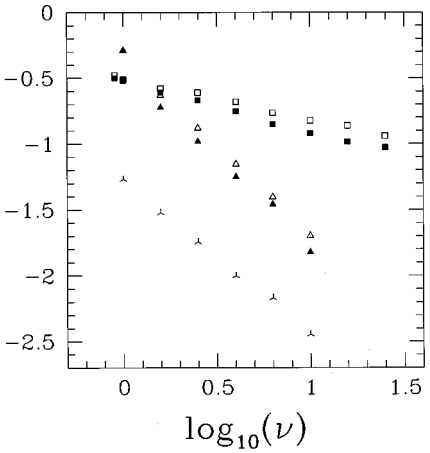

FIG. 6. $\log_{10}$-$\log_{10}$ plot of the variations with the spatial scaling factor ν of the relative difference $(\langle G\rangle - G)/G$ between a mean front property $\langle G\rangle$ and its deterministic prediction G for the two chemical models. Fisher model: (□) $G=E$ (profile width). (■) $G=V$ (propagation velocity). Schlögl model: (△) $G=E$ (profile width), (▲) $G=V$ (propagation velocity). (人) $G=a_{-\infty}$ (left plateau value, $G=\alpha$).

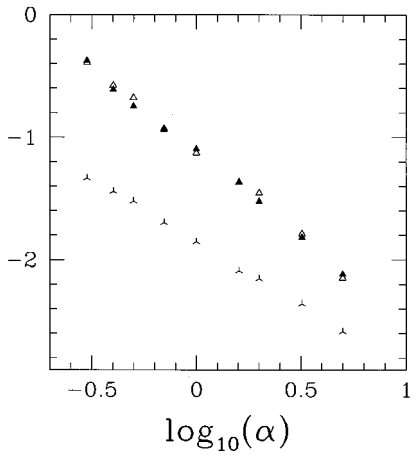

FIG. 7. $\log_{10}$-$\log_{10}$ plot of the variations with the stationary state value α of the relative difference $(\langle G\rangle - G)/G$ between a mean front property $\langle G\rangle$ and its deterministic prediction G for the Schlögl model: (△) $G=E$ (profile width). (▲) $G=V$ (propagation velocity). (人) $G=a_{-\infty}$ (left plateau value, $G=\alpha$).

relation between the fluctuation effects and the vicinity of the pitchfork bifurcation corresponding to $\alpha=\beta=\gamma=0$, in Fig. 7 we give a log-log plot of the variations with the parameter α of the relative difference between the mean front properties and the deterministic predictions. We obtain the following power laws:

$$\left(\frac{\langle E\rangle-\overline{E}}{\overline{E}}\right)_S \sim \left(\frac{1}{\alpha}\right)^{1.39\pm 0.02}, \tag{28}$$

$$\left(\frac{\langle V\rangle-\overline{V}}{\overline{V}}\right)_S \sim \left(\frac{1}{\alpha}\right)^{1.37\pm 0.02}, \tag{29}$$

$$\left(\frac{\langle a_{-\infty}\rangle-\alpha}{\alpha}\right)_S \sim \left(\frac{1}{\alpha}\right)^{1.02\pm 0.02}. \tag{30}$$

Comparing Figs. 6 and 7 for the Schlögl model, we observe deep analogies between the behaviors as $1/N$ and $1/\alpha$ vary. In both cases, we obtain very close values for the maximum deviation of velocity and width and a smaller value for the maximum deviation of the left plateau height. In Fig. 7, the exponent values associated with velocity and width, as the distance $1/\alpha$ from the bifurcation varies, are identical at the precision of the results. Their value also coincides with the value of the exponents determined in Fig. 6 as the system-size expansion parameter $1/N$ changes. Thus, in the case of a wave front propagating between two stable stationary states, the deviation between stochastic and deterministic predictions is a direct consequence of the well-known divergence of fluctuations in the vicinity of a bifurcation.

The different power laws characterizing the behavior of the deviations between the mean wave-front properties from their predictions by deterministic equations have been deduced for noise expressions given in Eqs. (17), (18), and (21), where the stochastic fraction a has been replaced by its deterministic value $\overline{a}$. In this approximation the noise in the leading edge of the front vanishes for the Fisher model and the Schlögl model with $\gamma=0$. We have checked that keeping the stochastic value a in the Langevin force expression of the Fisher model does not lead to any change [29]. For the Schlögl model with $\gamma=0$, the results given in Figs. 6 and 7 are not modified, and we obtain the same power laws for the propagation velocity, the profile width, and the left plateau height. Nevertheless, another fluctuation effect is observed on the right plateau height which reaches, in the permanent regime, a value different from $\gamma=0$. The deviation obeys a power law with the same exponent value, very close to 1, as the deviation of the left plateau height [33]. However, using the stochastic value a in the Langevin force expression of the Schlögl model with $\gamma\neq 0$ prevents us from studying the wave-front propagation. Actually, the noise induces a nucleation phenomenon [15,16,28], and the leading edge, initially prepared in the state γ, is destroyed before the passage of the wave. In other words, the internal fluctuations generate spontaneous transitions from the metastable stationary state γ to the other stable stationary state α, so that the right plateau does not reach a stationary value smaller than α.

V. CONCLUSION

The numerical resolution of the Langevin equations with specific internal noises deduced from master equations exhibits two qualitatively different behaviors for the wave fronts associated with cubic and quadratic chemical rates. In the case of a wave front between two stable stationary states, illustrated by the Schlögl model, the effect of fluctuations appears only in the vicinity of a bifurcation like the coalescence of the three stationary states. In these conditions, three qualitative effects may be observed: a marked increase of the propagation velocity and profile width, and a weaker decrease of the left plateau height. The variations of these effects with the fluctuation amplitude, controlled by the inverse of the system size, $1/N$, obey power laws associated with identical exponents, at the precision of our results. Very close behaviors are observed as the distance from the bifur-

cation changes. Obtaining exponent values greater than 1 proves that the fluctuation effects may be considered perturbative. Since the analytical expression of the deterministic profile and propagation velocity are known, a pure analytical study of the stochastic problem is consequently not hopeless. Work in this direction is in progress, one of the goals being the determination of a theoretical value for the exponents of the scaling laws associated with velocity and width.

The Fisher model illustrates a qualitatively different situation. Indeed, for wave fronts propagating into an unstable stationary state, the effect of fluctuations appears whatever the parameter values, and independently of the vicinity of a bifurcation. The plateau heights are absolutely not affected by the fluctuations. Their effects consist of an increase of the propagation velocity and the profile width. If the deviations for both quantities obey, as for the Schlögl model, power laws with close exponents, an important difference is the value of these exponents, much smaller than 1. Hence the effect of fluctuations cannot be considered as perturbative, and we believe that it is related to the existence of an infinite set of linearly stable solutions for the deterministic reaction-diffusion equation. In view of the nearly stable properties of the permanent solution of the Langevin equations when it is chosen as an initial condition of the deterministic equation, we conjectured [29] that the effect of fluctuations is to select a particular wave front in the continuum of possible deterministic solutions. Obtaining a qualitatively different behavior in the case of the Schlögl model that possesses a single wave-front solution, confirms this opinion. Unfortunately, an analytical study of the selection mechanism of a wave front in presence of fluctuations in the case of the Fisher model remains difficult to implement, especially because of the nonperturbative nature of the problem.

ACKNOWLEDGMENTS

This work was possible thanks to the support of the Institut de Développement et des Ressources en Informatique Scientifique (IDRIS, Orsay, France). We are grateful for financial support from the Action Intégrée TOURNESOL 96.038 between Belgium and France.

[1] P. C. Fife, *Mathematical Aspects of Reacting and Diffusing Systems*, Lecture Notes in Biomathematics Vol. 28 (Springer, Berlin, 1979).
[2] J. D. Murray, *Mathematical Biology* (Springer, Berlin, 1989).
[3] *Nonequilibrium Chemical Dynamics: From Experiment to Microscopic Simulations*, edited by F. Baras and D. Walgraef, special issue of Physica A **188** (1992).
[4] R. A. Fisher, Ann. Eugen. **7**, 335 (1937).
[5] A. Kolmogorov, I. Petrovsky, and N. Piskunov, Bull. Univ. Moscow Ser. Int. Sec. A **1**, 1 (1937).
[6] D. G. Aronson and H. F. Weinberger, Adv. Math. **30**, 33 (1978).
[7] W. van Saarloos, Phys. Rev. Lett. **58**, 2571 (1987).
[8] W. van Saarloos, Phys. Rev. A **37**, 211 (1988).
[9] W. van Saarloos, Phys. Rev. A **39**, 6367 (1989).
[10] F. Schlögl, C. Escher, and R. S. Berry, Phys. Rev. A **27**, 2698 (1983).
[11] L. Schimansky-Geier, A. S. Mikhailov, and W. Ebeling, Ann. Phys. (Leipzig) **40**, 277 (1983).
[12] G. Nicolis and I. Prigogine, *Self-Organization of Non-Equilibrium Systems* (Wiley, New York, 1977).
[13] N. G. van Kampen, *Stochastic Processes in Physics and Chemistry* (North-Holland, Amsterdam, 1980).
[14] G. W. Gardiner, *Handbook of Stochastic Methods* (Springer, Berlin, 1985).
[15] A. Lawniczak, D. Dab, R. Kapral, and J.-P. Boon, Physica D **47**, 132 (1991).
[16] D. Gruner, R. Kapral, and A. Lawniczak, J. Chem. Phys. **99**, 3938 (1993).
[17] B. Chopard and M. Droz, Europhys. Lett. **15**, 459 (1991).
[18] S. Cornell, M. Droz, and B. Chopard, Phys. Rev. A **44**, 4826 (1991).
[19] B. Chopard, M. Droz, T. Karapiperis, and Z. Racz, Phys. Rev. E **47**, R40 (1993).
[20] A. Lemarchand, A. Lesne, A. Perera, M. Moreau, and M. Mareschal, Phys. Rev. E **48**, 1568 (1993).
[21] A. Lemarchand, H. Lemarchand, A. Lesne, and M. Mareschal, in *Far From Equilibrium Dynamics of Chemical Systems*, edited by J. Gorecki *et al.* (World Scientific, Singapore, 1994).
[22] A. Lemarchand and M. Mareschal, in *Computer Simulation in Materials Science*, edited by H. O. Kirchner *et al.* (Kluwer, Dordrecht, 1996), p. 259.
[23] M. A. Burschka, C. R. Doering, and D. ben-Avraham, Phys. Rev. Lett. **63**, 700 (1989).
[24] J. Riordan, C. R. Doering, and D. ben-Avraham, Phys. Rev. Lett. **75**, 565 (1995).
[25] H. P. Breuer, W. Huber, and F. Petruccione, Physica D **73**, 259 (1994).
[26] H. P. Breuer, W. Huber, and F. Petruccione, Europhys. Lett. **30**, 69 (1995).
[27] A. Lemarchand, H. Lemarchand, E. Sulpice, and M. Mareschal, Physica A **188**, 277 (1992).
[28] G. F. Mazenko, O. T. Valls, and P. Ruggiero, Phys. Rev. B **40**, 384 (1989).
[29] A. Lemarchand, A. Lesne, and M. Mareschal, Phys. Rev. E **51**, 4457 (1995).
[30] A. Lemarchand, I. Nainville, and M. Mareschal (unpublished).
[31] J. Crank, *The Mathematics of Diffusion* (Clarendon, Oxford, 1975).
[32] G. A. Bird, *Molecular Gas Dynamics and the Direct Simulation of Gas Flows* (Clarendon, Oxford, 1994).
[33] M. A. Karzazi (unpublished).